Electronic Supplementary Material (ESI) for Lab on a Chip.

Supplementary Information for:

Customisable 3D Printed Microfluidics for Integrated Analysis and Optimisation

T. Monaghan[a], M. J. Harding[b], S. D. R. Christie[b], R. A. Harris[a] and R. J. Friel[a]

[a] School of Mechanical and Manufacturing Engineering, Loughborough University, Ashby Rd, Loughborough, LE11 3TU, United Kingdom

[b] Department of Chemistry, Loughborough University, Loughborough, Ashby Road, Leicestershire, LE11 3TU, United Kingdom

Author contact information: t.monaghan@lboro.ac.uk

Table of Contents

Contents	Pages No.
General	1
Design of Experiments Data	1-5
Device Characterisation and Performance	5-10
Transmission Performance Spectral Data	10
Schematic Images of 3D Mixing Device	11

General. All reagents and solvents were used as received. In order to measure both the optical fibre performance and monitor the proceeding reactions, a deuterium-halogen light source (DH-2000, Ocean Optics, Oxford, UK) and an S2000 UV/Vis spectrometer with a USB1000-ADC analogue to digital converter (Ocean Optics) were employed. These were connected to the embedded optical fibres via the use of a multi-mode SMA connector (Newport Spectra-Physics Ltd, Oxford, UK).

Design of Experiments Data.

Model Reaction

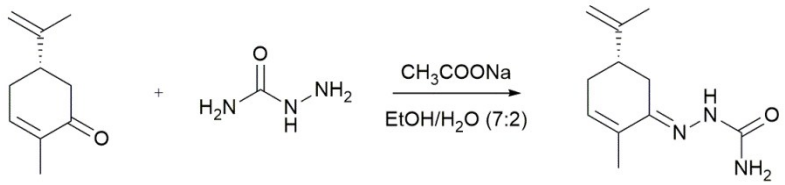

Table 1. Conditions Screened

Variable	Low	Medium	High
Temperature [^{o}C]	120	140	160
Residence Time [min]	25	33.3	50

Reaction optimisation was performed using a response surface methodology (RSM), central composite faced (CCF) design of experiments (DOE) approach and continuous monitoring of the reaction UV spectrum via integrated optical fibres.

Table 2. DOE Results

All experiments were randomized in order to balance the effect of extraneous or uncontrollable conditions that could impact the results of the experiment e.g. ambient temperature, humidity which can change during an experiment and inadvertently affect test results. By randomizing the order in which experimental runs are done, it is possible to reduce the probability that differences in experimental conditions or materials strongly bias results.

Experiment No.	Run Order	Equivalents	Temperature	Residence time	UV_265
1	5	2	108	25	0.509335
2	11	2	140	25	0.586103
3	10	2	108	50	0.772425
4	3	2	140	50	0.837296
5	6	2	108	33.3	0.690323
6	9	2	140	33.3	0.77795
7	4	2	120	25	0.51263
8	2	2	120	50	0.797592
9	8	2	120	33.3	0.684597
10	1	2	120	33.3	0.712399
11	7	2	120	33.3	0.709135

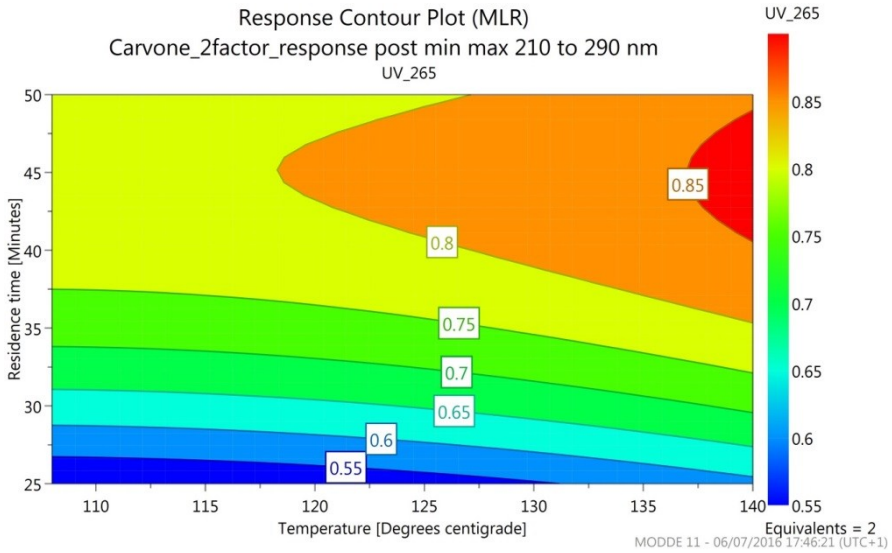

S.1. Response Contour Plot (RCP) for the optimisation DOE for a) product and b) starting material

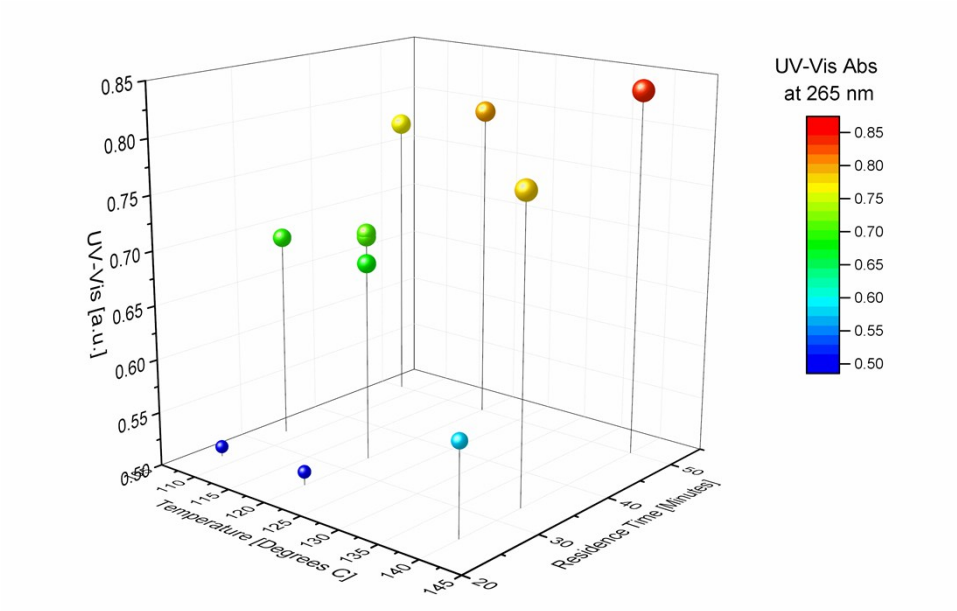

S.2. Ball and Stick diagram for individual responses in the DOE

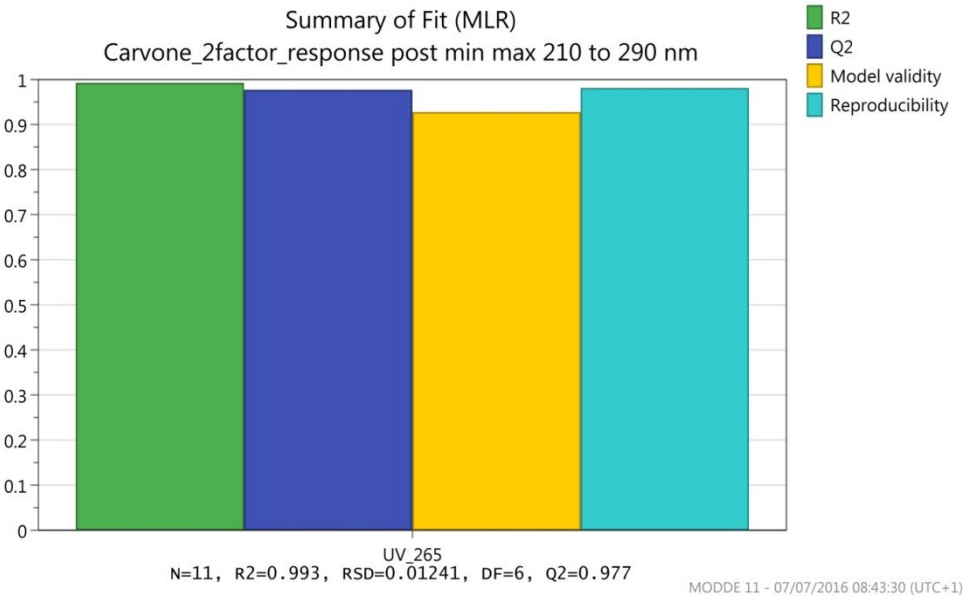

S.3. Summary of fit information for DOE model

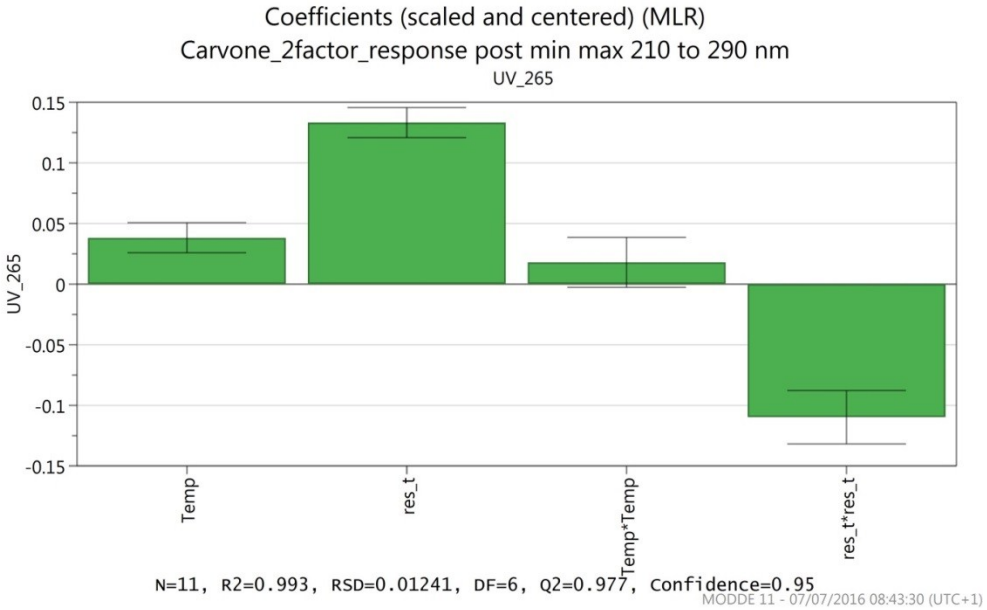

S4. Coefficients for model generated from DOE results

S.4. Coefficient list for product and starting material plots

UV_265	Coeff. SC	Std. Err.	P	Conf. int(±)
Constant	0.769932	0.00751573	5.83128e-011	0.0183905
Temperature	0.0382111	0.0050681	0.000282295	0.0124013
Residence time	0.133207	0.0050681	2.00145e-007	0.0124013
Temp*Temp	0.0179155	0.00842868	0.0776859	0.0206244
res_t*res_t	-0.109835	0.00899937	1.84119e-005	0.0220208

N = 11	Q2 =	0.977	Cond. no. =	3.823
DF = 6	R2 =	0.993	RSD =	0.01241
	R2 adj. =	0.988		
			Confidence =	**0.95**

All summary terms are of suitable magnitude to suggest that the DOE model generated is not just acceptable, but is excellent and can be used with a high degree of reliability and predictability. Data suggest that higher temperatures and moderate residence times are favourable for achieving high degrees of product conversion. P values indicate that the model is predominately linear, as the squared term Temp*Temp is greater than 0.05 and therefore its 2nd order effects are insignificant. Removal of the res_t*res_t term has a detrimental effect on the models predictive power and was therefore included in the response surface model.

Information on Device Characterisation and Performance

Located below are a series of images and data to indicate further device characterisation and performance testing which is referred to in the main body of the article.

Pressure Sensitive Adhesive Film Characterisation

Several commercially available PSA films were trailed in order to establish which was most suitable for the sealing of microfluidic channel networks. The most suitable testing for the various tapes was based upon their mechanical performance and performance under flow conditions. As a result, mechanical peel testing was carried out in accordance with pressure testing as well as examining the tapes ability to cope sealing fluidic channels at varying flow rates. The details of these tests are located in S.5.

S.5. Information on chosen tapes

Tape Model	*Manufacturer*	*Description*	*Abbreviation in this work*
254m	ADCHEM	Double coated PET carrier film with acrylic adhesive	ADC - 254
4965	Tesa® Tapes	Double coated PET carrier film with acrylic adhesive	T - 4965
4959	Tesa® Tapes	Non-woven carrier with a tackified acrylic adhesive	T - 4659
8914	Adhesive Research Inc.	Double coated polyester carrier with acrylic adhesive	AR - 8914
OMF	DTLSupplies Ltd.	Double coated polyester with acrylic adhesive	DTL - OMF
DSMF	DTLSupplies Ltd.	Double coated PVC carrier with acrylic adhesive	DTL - DSMF

Mechanical Peel Testing:

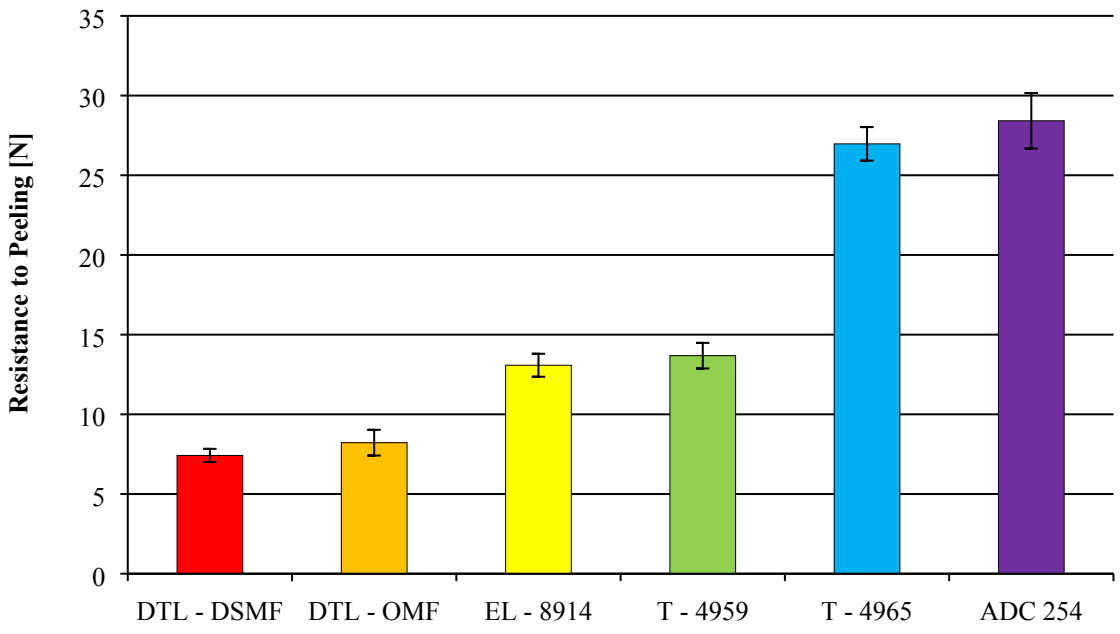

S.6. Resistance to peeling of the selected tapes

*all peel testing was performed in accordance with ASTM D3330 using an Instron 3366 tensile test machine (Instron®, UK) fitted with a 100 N load cell

Flow Performance Testing:

To ensure that the newly formed devices were capable of accommodating the flow rates required of microfluidic devices, flow performance testing was performed. In order to measure the flow performance of the additively manufactured device, a T-mixer was designed and manufactured prior to connection to the FlowSyn system – Figure x. After connection to the pumping equipment, water was pumped through the device at increasing flow rates via the two incorporated inlets. The flow rate at each pump started at 1ml/min and increased by 1ml/min until a maximum total flow rate of 10 ml/min was reached.

All tapes were able to tolerate these flow rates without demonstrating any degree of tape lift off or leakage.

Pressure Testing:

Pressure testing of the tapes was achieved through the use of a test piece in which solvent was allowed to flow to the surface of a test part into a dead-end channel, allowing gradual pressure build up within the system until eventual tape failure.

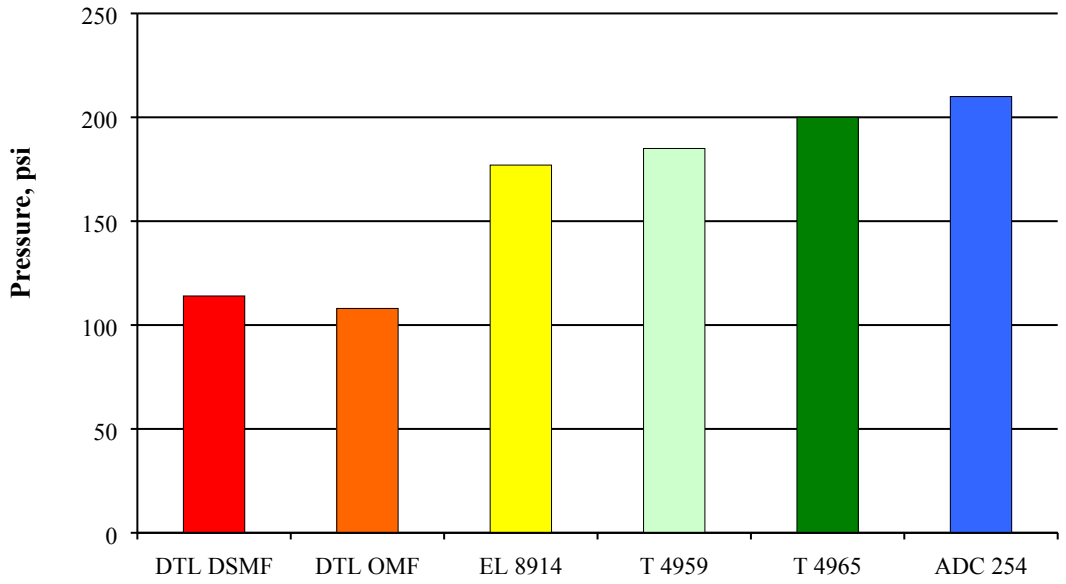

S.7 The average pressure achieved for each tape prior to failure

Solvent Testing:

From the information gained in these early trails, the T-4965 tape was chosen for further testing. This involved subjecting the tape to various organic solvents at a flow rate of 1 ml min^{-1} in order to see if there was any observed degradation of the overlying laminar structure.

S.8. Solvent compatibility of overlying adhesive layer

Solvent	**Effect on Tape**
Toluene	Substantial tape lift off over channel
Isopropyl Alcohol (IPA)	No effect
Hexane	Minimal tape lift
Light Petrol	Moderate tape lift
Water	No effect
Ethyl Acetate	Minimal tape lift
Diethyl Ether	Minimal tape lift
Acetonitrile	No effect

Channel Quality Assessment:

The images located below are intended to highly the increased channel quality which can be brought about using the methods detailed in the accompanying article.

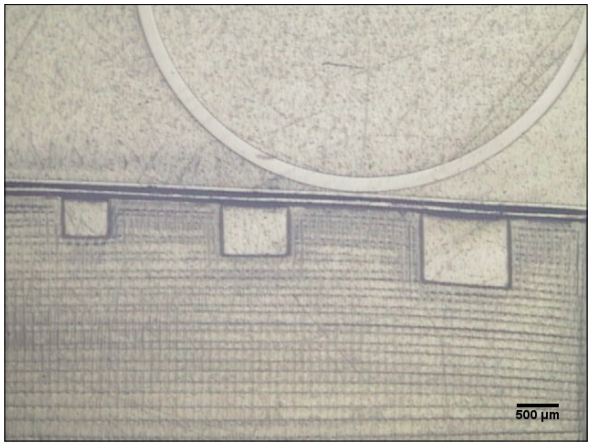

S.9 In-line view of surface channels sealed with PSA layer showing high channel quality and lack of stair stepping

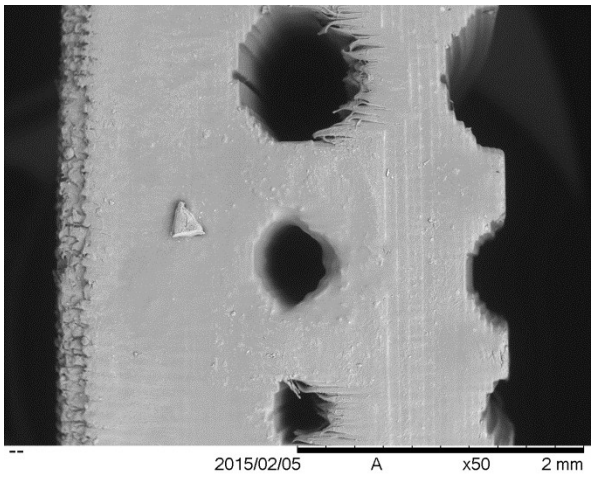

S.10. SEM image to show issues associated with the manufacture of circular internal and surface channels e.g. the distortion of unsupported channel ceilings in internal features as well as stair stepping in both internal and surface channels.

Flow regime within channels

Using the methods described in this paper for both the production and sealing of fluidic channels, two simple test devices were designed and manufactured. One simple device to establish if the system exhibited laminar flow between passing solutions, and another to establish if more complex fluid manipulation could be achieved. These came in the form of a simple Y-mixer with a proceeding serpentine channel and also a hydrodynamic focussing device. These devices were infused with dye solutions (Rhodamine B and Methylene Blue) and imaged via optical microscopy. Located below are the resulting images:

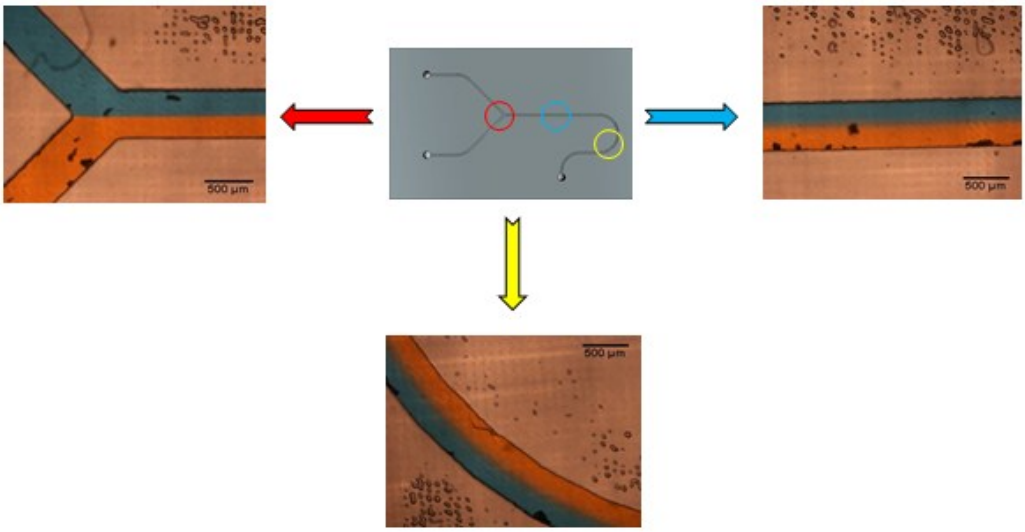

S.11. Images of Y-mixer and serpentine channel path demonstrated high degrees of laminar flow throughout

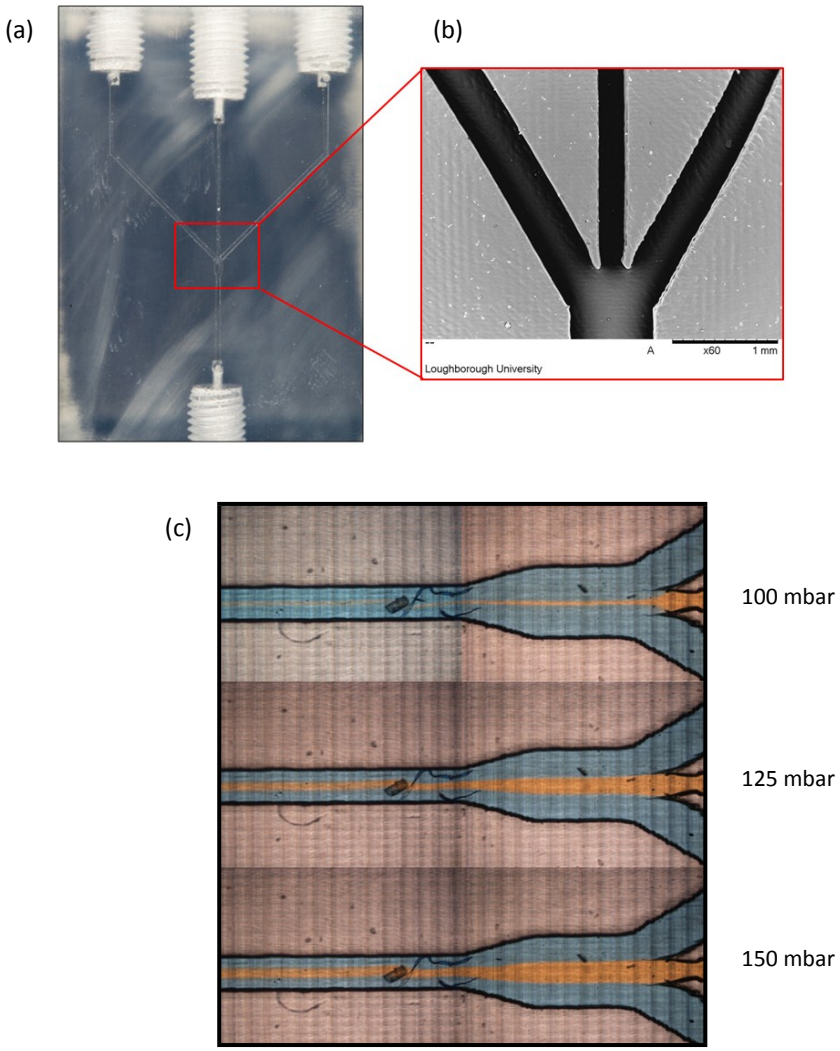

S.12. (a) Optical and (b) SEM images of hydrodynamic focussing device along with (c) optical images to show the devices focussing ability using different core stream pressures

Information regarding the transmission performance of

various fibre combinations

The spectral counts recorded for each of the various fibre combinations is located below.

S.13. Transmission intensity of various optical fibre combinations at 265nm

Fibre Combination	10 ms acquisition at 265 nm / counts	100 ms acquisition at 265 nm / counts
A - B (**1**)	178.143	1730.57
B - A (**2**)	166.286	1598.71
B - B (**3**)	138.429	1307.43
A - A (**4**)	92.571	587.571

* The first fibre listed was used as the transmitting fibre whilst the second fibre was acting as the collecting fibre e.g. in B-A combinations, fibre B was connected to the light source and A the spectrometer

Schematic Images of 3D Mixing Device used for Optimisation DOE:

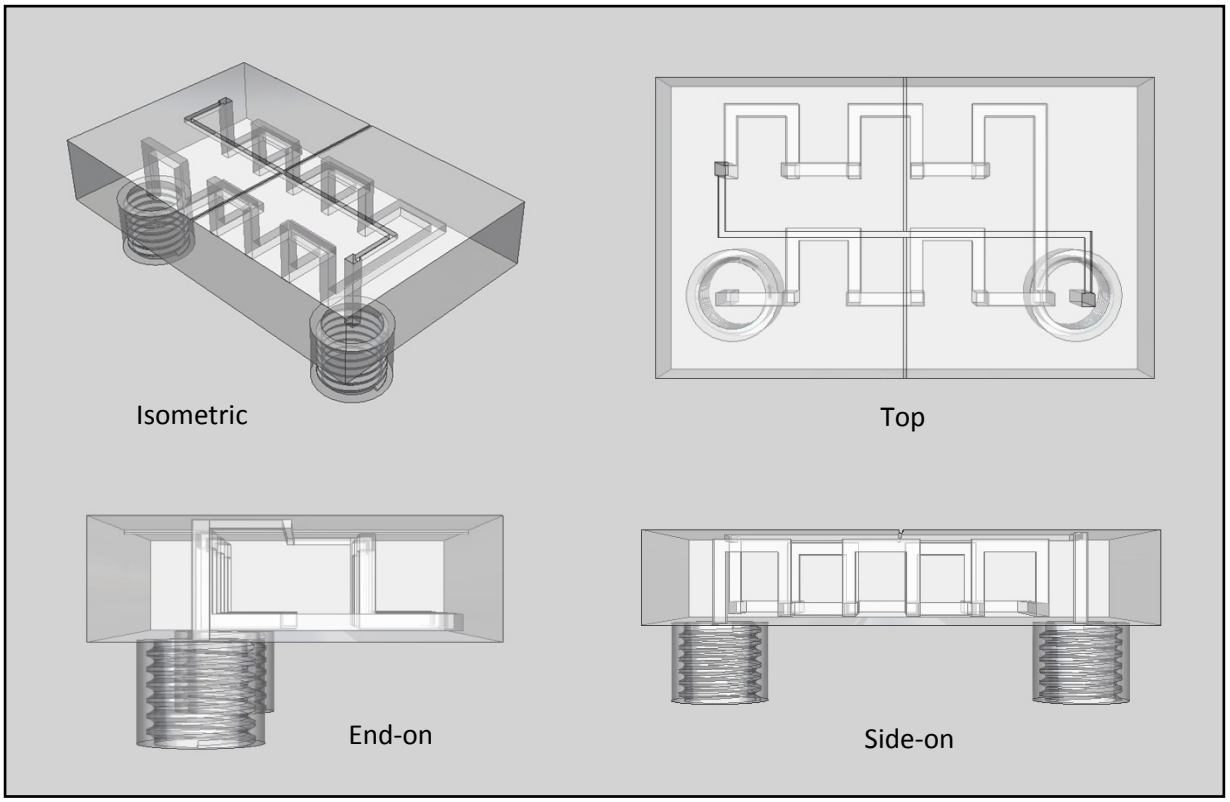

S.14. various orientations of the complex mixing device used in the optimisation experiments for the carvone semicarbazone